THE JOURNAL OF PHYSICAL CHEMISTRY B

Article

pubs.acs.org/JPCB

Influence of Alkyl Chain Length and Temperature on Thermophysical Properties of Ammonium-Based Ionic Liquids with Molecular Solvent

T. Kavitha,[†] Pankaj Attri,[‡] Pannuru Venkatesu,*[,‡] R. S. Rama Devi,[†] and T. Hofman[§]

[†]Department of Chemistry, Sri Padmavathi Womens Degree and Post Graduate College, Tirupati 517 502, India

[‡]Department of Chemistry, University of Delhi, Delhi 110 007, India

[§]Division of Physical Chemistry, Warsaw University of Technology, ul. Noakowskiego 3, 00-664 Warszawa, Poland

Supporting Information

ABSTRACT: Mixing of ionic liquids (ILs) with molecular solvent can expand the range of structural properties and the scope of molecular interactions between the molecules of the solvents. Exploiting of these phenomena essentially require a basic fundamental understanding of mixing behavior of ILs with molecular solvents. In this context, a series of protic ILs possessing tetra-alkyl ammonium cation $[R_4N]^+$ with commonly used anion hydroxide $[OH]^-$ were synthesized and characterized by temperature dependent thermophysical properties. The ILs $[R_4N]^+[OH]^-$ are varying only in the length of alkyl chain (R is methyl, ethyl, propyl, or butyl) of tetra-alkyl ammonium on the cationic part. The ILs used for the present study included tetramethyl ammonium hydroxide $[(CH_3)_4N]^+[OH]^-$ (TMAH), tetraethyl ammonium hydroxide $[(C_2H_5)_4N]^+[OH]^-$ (TEAH), tetrapropyl ammonium hydroxide $[(C_3H_7)_4N]^+[OH]^-$ (TPAH) and tetrabutyl ammonium hydroxide $[(C_4H_9)_4N]^+[OH]^-$ (TBAH). The alkyl chain length effect has been analyzed by precise measurements such as densities (ρ), ultrasonic sound velocity (u), and viscosity (η) of these ILs with polar solvent, *N*-methyl-2-pyrrolidone (NMP), over the full composition range as a function of temperature. The excess molar volume (V^E), the deviation in isentropic compressibility ($\Delta\kappa_s$) and deviation in viscosity ($\Delta\eta$) were predicted using these properties as a function of the concentration of ILs. Redlich–Kister polynomial was used to correlate the results. A qualitative analysis of the results is discussed in terms of the ion-dipole, ion-pair interactions, and hydrogen bonding between ILs and NMP molecules. Later, the hydrogen bonding features between ILs and NMP were also analyzed using a molecular modeling program with the help of HyperChem 7.

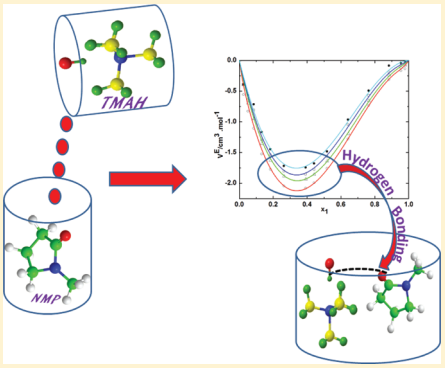

1. INTRODUCTION

In recent years, large quantities of solvents have been used for numerous processes in academia and industries. However, because of new environmental regulations, the challenge of using nonharmful solvents has prompted a great of development of innovative products to protect the environment. In this context, ionic liquids (ILs) emerged as a new class of solvents considered for the replacement of volatile organic compounds in chemical processes to reduce both cost and environmental pollution.[1−4] The IL completely consists of the weak coordinating of ions such as an organic cation and the inorganic or organic anion.[5,6] The potential utilization and applications of ILs have been rapidly increased in all scientific fields by several researchers.[7−16] Apparently, the physicochemical properties of ILs are quite sensitive toward the structure and nature of cations and anions.[17,18] The variations in thermophysical properties of ILs, such as density (ρ), speed of sound (u), viscosity (η), and conductivity, are observed to be very sensitive to the change in cation, mainly due to microscopic level interactions between solvent molecules.[19]

Obviously, an interesting aspect is that ILs being able to influence on physicochemical properties of mixtures and even a

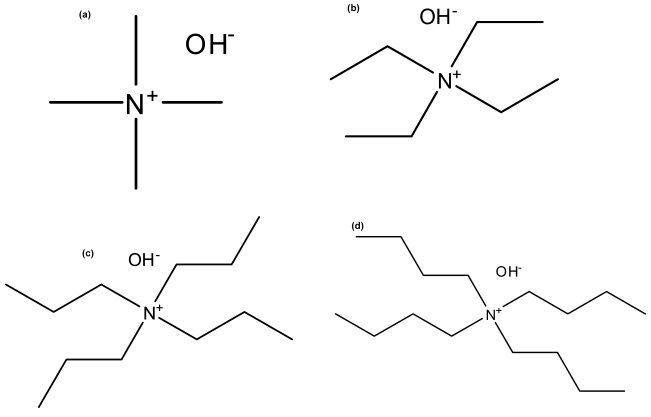

Figure 1. Schematic structures for ILs such as (a) TMAH, (b) TEAH, (c) TPAH, and (d) TBAH.

Received: February 15, 2012
Revised: March 22, 2012
Published: March 24, 2012

slight variation in their ions that can lead substantial differences in their properties. However, very little work is known about the appropriate variation in physicochemical properties upon varying either an anion or the cation in ILs. The experimental values of thermophysical properties allow us establishing new predictive interactions and information about the molecular level structure of the mixtures to determinate the properties that are necessary for the industry in a fast reliable and economical way. Therefore, a deep knowledge of thermophysical properties of liquid mixtures containing ILs has essentially required for scientific community.

N-Methyl-2-pyrrolidone (NMP) is a dipolar aprotic basic solvent that is frequently used to recover hydrocarbons from petrochemical processes by extractive distillation. Moreover, NMP has large chemical and thermal resistance, low toxicity, and high selectivity.[20] NMP is also used as an extractive agent for paraffin and aromatic separations. Nowadays, the demand for the NMP is explicitly and incessantly increasing with the research and development of the electronics and chemical industry. It has a large dipole moment (μ = 4.09 D) and a high dielectric constant (ε = 32.2 at T = 298.15 K).[21] Moreover, NMP is a strong polar liquid and has the potential for use in the solvent extraction process for separating polar substances from nonpolar substances.[22,23]

This work is a part of our extensive ongoing project aimed at a detailed characterization of ILs in molecular solvents and in biomolecules.[6,8,12−16] Here, we now uncover the characterization for the structural variation of cations of ammonium based ILs as well as molecular interactions with a molecular solvent through temperature variable properties. Studies on thermophysical properties of the pure ILs and their mixtures with polar compounds have shown that the choice of anion or cation has strongly influenced on the molecular properties of different ILs.[12−15,24] The knowledge of thermophysical properties of mixed solvents of ILs with organic molecular liquid are paramount for the design of many technological processes and required for many practical applications.[24−27] In spite of the importance of properties of ILs in different solvent media, only a small amount of physicochemical data is available in the literature, which mainly characterizes ILs.[28−35] A survey of the literature reveals that thermophysical properties of pure ILs

Table 1. Solvent Molecular Weight (MW), Purity, Density (ρ), Speed of Sound (u), and Viscosity (η) for the Solvents Such As ILs and NMP at 298.15 K

solvent	MW (g mol^{-1})	purity (%)	ρ/(g cm^{-3})	u/(m s^{-1})	η/(mPa s)
NMP	99.13	99	1.02590[a,b]	1552[c,f]	1.66[g]
			1.02374[c,d,e]		1.49[c,h]
TMAH	99.15	99	1.01797	1828	2.77
TEAH	147.26	99	1.00881	1814	4.94
TPAH	203.37	99	0.99594	1801	6.10
TBAH	259.50	99	0.99358	1798	6.69

[a]1.02590 from ref 21. [b]1.025590 from ref 36. [c]At 303.15 K. [d]1.02370 from ref 21. [e]1.02395 at 303.15 K, from ref 38. [f]1527 at 303.15 K, from ref 38. [g]1.66 from ref 21. [h]1.55 at 303.15 K, from ref 38.

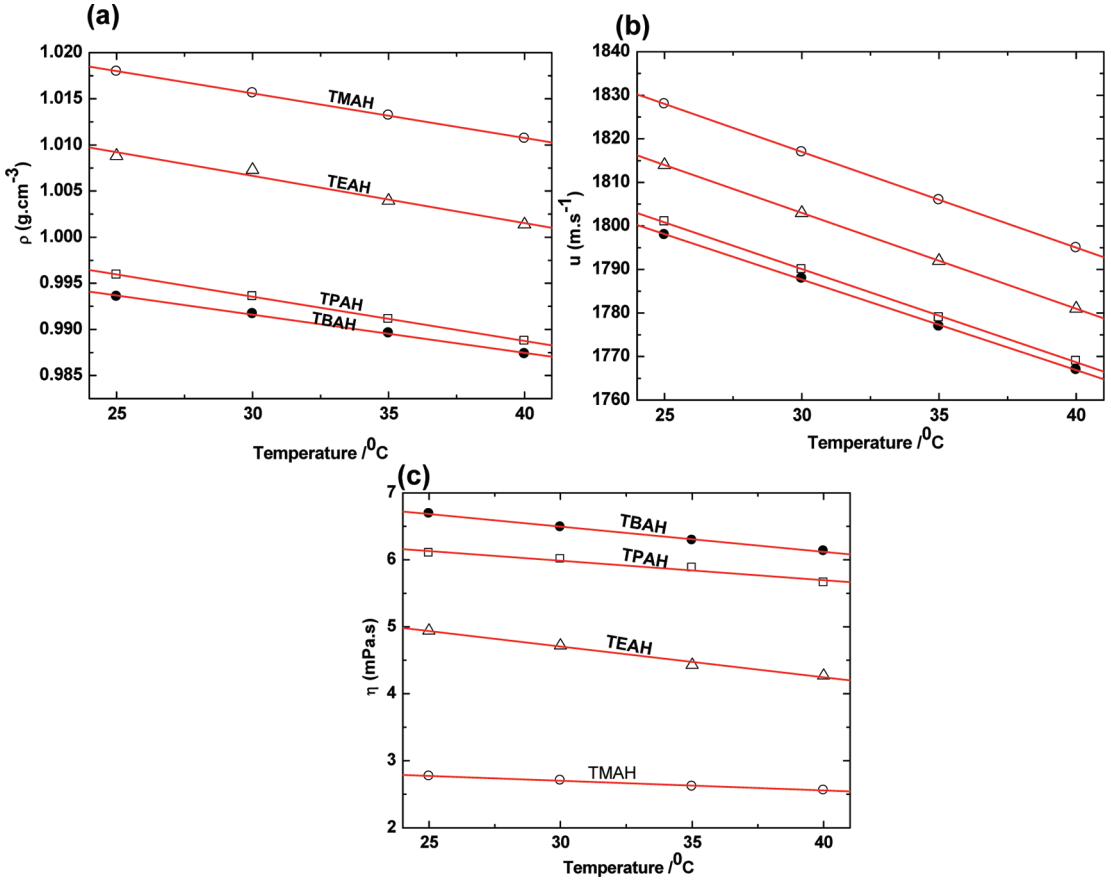

Figure 2. Influence of alkyl-chain length on (a) density, (b) ultrasonic sound velocity, and (c) viscosity for ammonium based ILs: (○) TMAH, (Δ) TEAH, (□) TPAH, and (●) TBAH plotted against temperatures.

dx.doi.org/10.1021/jp3015386 | J. Phys. Chem. B 2012, 116, 4561−4574

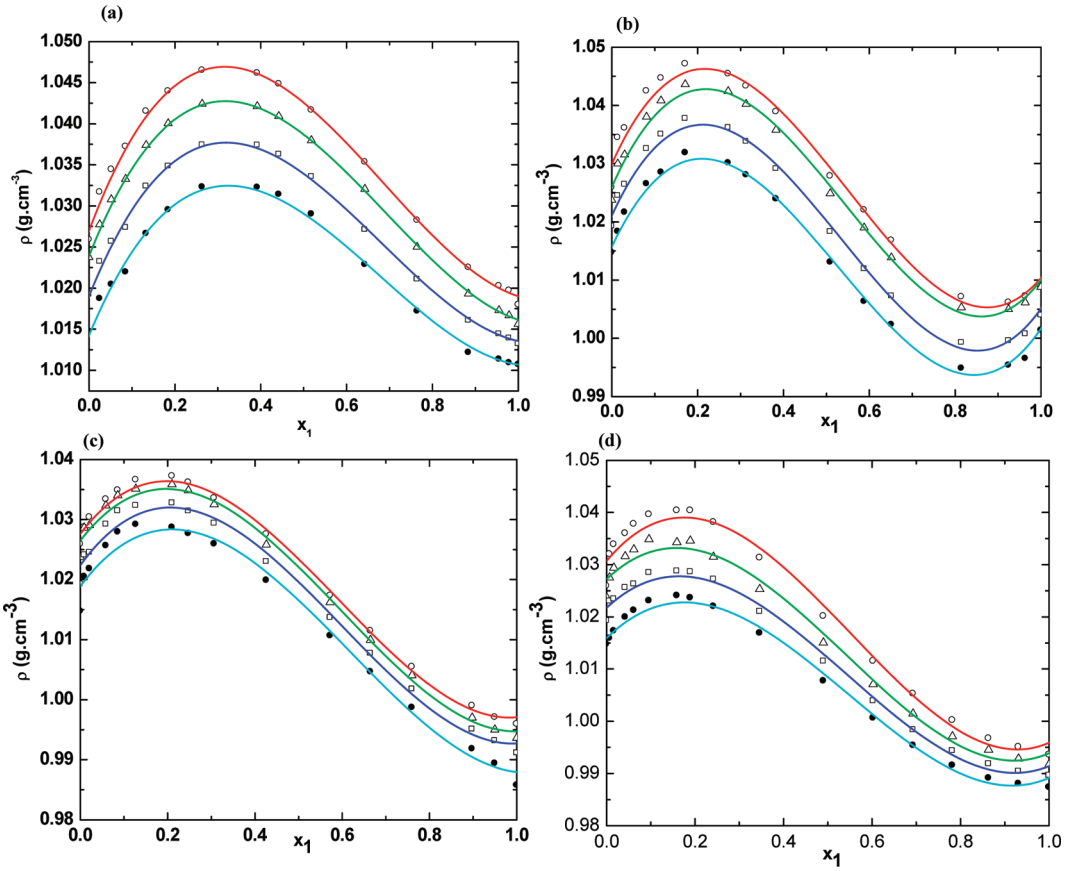

Figure 3. Densities (ρ) for the mixtures of ILs + NMP as a function of the composition expressed in the mole fraction (x_1) of IL for (a) TMAH (1) + NMP (2); (b) TEAH (1) + NMP (2); (c) TPAH (1) + NMP (2); and (d) TBAH (1) + NMP (2) at (○) 25, (Δ) 30, (□) 35, and (●) 40 °C at atmospheric pressure. The solid line represents the smoothness of these data.

have been reported extensively implying widespread interest from both fundamental and industrial points of view. However, the thermophysical properties of ILs particularly in molecular solvents have not been explored in a systematic way. In this context, our aim is to explore thermophysical properties such as ρ, u, and η for the mixed solvents of ILs and polar solvent to expand the basic needs for scientific research. Further, to gain some insight into several aggregations of molecular interactions of ILs with polar compounds, we have synthesized the ILs of different combination of cations with commonly used anion for our study because these novel kinds of ILs appear to be promising for various applications for the chemical community.

The main goal of the work is to report molecular and structural information between ILs and NMP based on the temperature dependence properties of ρ, u, and η as well as derived properties of excess molar volume (V^E), deviation of isentropic compressibility ($\Delta\kappa_s$), and deviation in viscosity ($\Delta\eta$). We report here the synthesis of tetramethyl ammonium hydroxide $[(CH_3)_4N]^+[OH]^-$ (TMAH), tetraethyl ammonium hydroxide $[(C_2H_5)_4N]^+[OH]^-$ (TEAH), tetrapropyl ammonium hydroxide $[(C_3H_7)_4N]^+[OH]^-$ (TPAH), and tetrabutyl ammonium hydroxide $[(C_4H_9)_4N]^+[OH]^-$ (TBAH). A survey of the literature reveals that no studies of V^E, $\Delta\kappa_s$, and $\Delta\eta$ are reported for ammonium ILs with NMP. In this paper, we report the measured results of ρ, u, and η for the mixtures of ILs with NMP over a complete mole fraction range at 5 °C intervals over a wide temperature range of 25 − 40 °C. Moreover, the hydrogen bonding features between ILs and NMP were carried out to get deeper insight into intermolecular interactions for the studied compounds. These studies were performed according to the semiempirical calculations by using Hyperchem 7.

2. EXPERIMENTAL SECTION

2.1. Materials. NMP (Merck >99% of purity) was stored over freshly activated 3 Å molecular sieves and was purified by the standard method described by Riddick et al.[21] The purity of the NMP was verified by measuring the ρ, u, and η which were in good agreement with the literature values.[21,36−38] The purity of the sample was further confirmed by GLC single sharp peaks. To our knowledge, the values of ρ, u, and η for studied ammonium ILs are not available in the open literature, and a data of comparison for the values of ILs could not be drawn in the present study. The ILs used in the present study were synthesized in our laboratory, as given below.

2.2. Synthesis of ILs. Ammonium based protic ILs used in this study, abbreviated as TMAH, TEAH TPAH, and TBAH, were synthesized[14,39,40] by the procedure as follows.

2.2.1. Synthesis of Tetramethyl Ammonium Hydroxide (TMAH). The synthesis of this IL was carried out in a 250 mL round bottomed flask, which was immersed in a water-bath and fitted with a reflux condenser. Solid potassium hydroxide (40 mmol) was added to a solution of tetramethyl ammonium bromide $[(CH_3)_4N]^+[Br]^-$ (40 mmol) in dry methylene chloride (20 mL), and the mixture was stirred vigorously at room temperature for 10 h. The precipitated KBr was filtered off, and the filtrate was evaporated to leave the crude $[(CH_3)_4N]^+[OH]^-$ as a viscous liquid that was washed with ether (2 × 20 mL) and dried at 70 °C for 5 h to obtain the pure IL. The sample was analyzed

dx.doi.org/10.1021/jp3015386 | J. Phys. Chem. B 2012, 116, 4561−4574

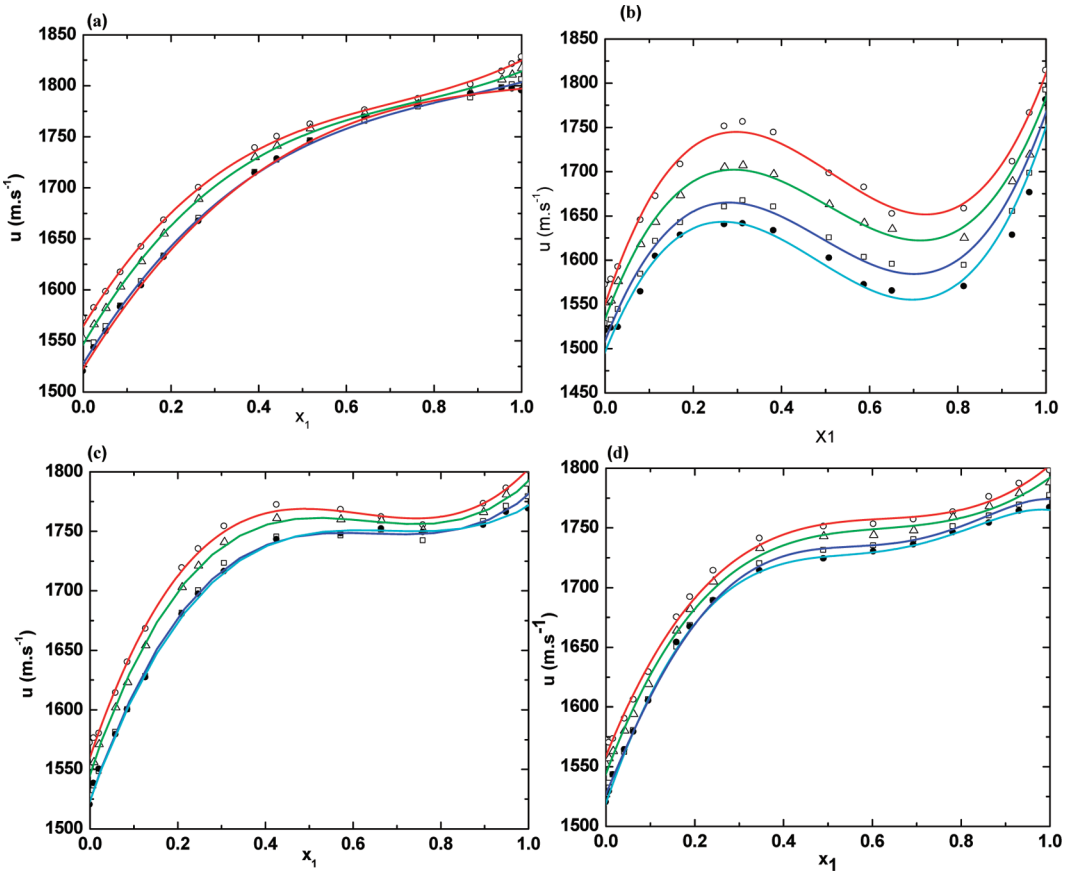

Figure 4. Ultrasonic sound velocity (u) for the mixtures of ILs + NMP as a function of the composition expressed in the mole fraction (x_1) of IL for (a) TMAH (1) + NMP (2), (b) TEAH (1) + NMP (2), (c) TPAH (1) + NMP (2), and (d) TBAH (1) + NMP (2) at (○) 25, (Δ) 30, (□) 35, and (●) 40 °C at atmospheric pressure. The solid line represents the smoothness of these data.

by Karl Fisher titration and revealed very low levels of water (below 70 ppm). The yield of TMAH was 68%. ^{1}H NMR (DMSOd_6): δ (ppm) 2.38 (s, 12H), 4.79 (s, OH). HRMS calculated for $C_4H_{13}NO$ (M + −OH) 91.15, found 91.09.

2.2.2. Synthesis of Tetraethyl Ammonium Hydroxide (TEAH). A similar procedure as delineated above for $[(C_2H_5)_4N]^+[OH]^-$ was followed with the exception of the use of $[(C_2H_5)_4N]^+[Br]^-$ ([cation]) instead of $[(CH_3)_4N]^+[Br]^-$. The yield of TEAH was 78%. ^{1}H NMR (DMSOd_6): δ (ppm) 1.01 (t, 12H), 3.06 (q, 8H), 4.43 (s, OH). HRMS calculated for $C_8H_{21}NO$ (M+ - OH) 147.26, found 147.20.

2.2.3. Synthesis of Tetrapropyl Ammonium Hydroxide (TPAH). A procedure similar to that above for $[(CH_3)_4N]^+[OH]^-$ was followed with the exception of the use of $[(C_3H_7)_4N]^+[Br]^-$ ([cation]) instead of $[(CH_3)_4N]^+[Br]^-$. The yield of TPAH was 82%. ^{1}H NMR (DMSOd_6): δ (ppm) 0.8 (t, 12H), 1.46 (m, 8H), 2.92 (t, 8H), 4.56 (s, OH). HRMS calculated for $C_{12}H_{29}NO$ (M + −OH) 203.36, found 203.25.

2.2.4. Synthesis of Tetrabutyl Ammonium Hydroxide (TBAH). A procedure similar to that above for $[(CH_3)_4N]^+[OH]^-$ was followed with the exception of the use of $[(C_4H_9)_4N]^+[Br]^-$ ([cation]) instead of $[(CH_3)_4N]^+[Br]^-$. The yield of TBAH was 82%. ^{1}H NMR (DMSOd_6): δ (ppm) 0.94 (t, 12H), 1.37 (m, 8H), 1.96 (m, 8H), 3.43 (t, 8H), 4.78 (s, OH). HRMS calculated for $C_{16}H_{37}NO$ (M + −OH) 259.47 found 259.34.

All ILs were degassed and dried over 3 Å molecular sieves and the purity of ILs was confirmed by ^{1}H NMR analysis as well as GLC single sharp peaks. ^{1}H (400 MHz) spectra were recorded on a JEOL 400 NMR spectrometer in DMSO-d_6. The schematic chemical structures of ILs are shown in Figure 1. The molecular weight, normal purity, ρ, u, and η of ILs and NMP, which are studied in the present work, are summarized in Table 1.

2.3. Methods. *2.3.1. Sample Preparation.* Clear binary mixtures were prepared by weighing the components using a Mettler Toledo balance with an accuracy of ±0.0001 g for all measurements. The estimated uncertainty on the mole fraction composition was found to be less than 5×10^{-4}. Mixing of the two components was promoted by the movement of a small glass sphere (inserted in the vial prior to the addition of the ILs) as the flask was slowly and repeatedly inverted. After mixing the sample, the bubble-free homogeneous sample was transferred into the U-tube of the densimeter or the sample cell of ultrasonic interferometer through a medical syringe. A bubble-free sample was introduced into the sample cell, and the cell was placed under the sensor plates of the viscometer.

2.3.2. Density Measurements. The density measurements of various ILs, NMP, and ILs + NMP were carried out using an Anton-Paar DMA 4500 M vibrating-tube densimeter, equipped with a built-in solid-state thermostat and a resident program with accuracy of temperature of ±0.03 °C. The uncertainties in the density experimental measurements were ±0.00005 g cm^{-3}. The instrument was calibrated once a day with double distilled, deionized water and with air at 20 °C as standards. The excess molar volumes (V^E) of ILs with NMP systems over the IL concentration range at different temperatures have been deduced from the ρ of the pure compounds and mixture (ρ_m) using the standard equations.[24]

dx.doi.org/10.1021/jp3015386 | J. Phys. Chem. B 2012, 116, 4561−4574

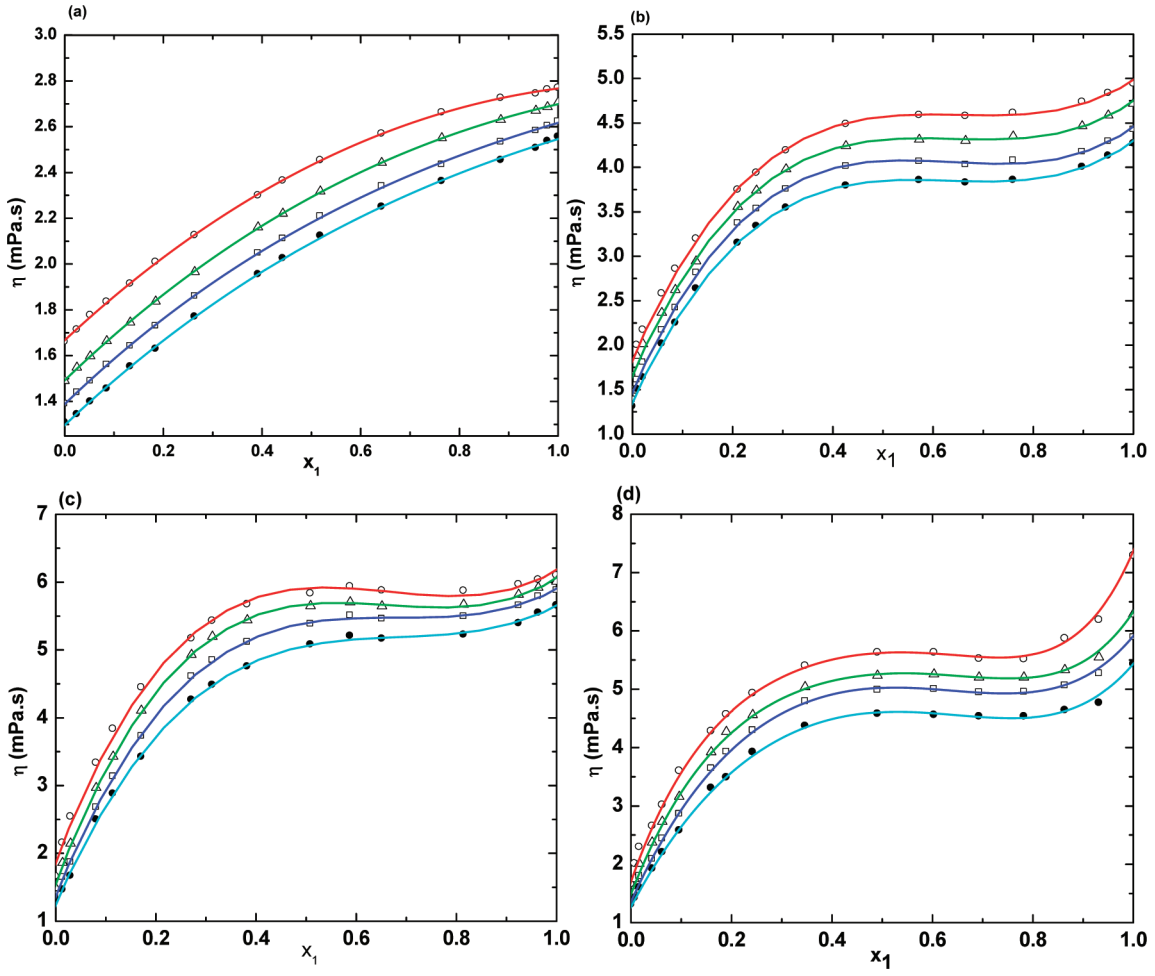

Figure 5. Viscosities (η) for the mixtures of ILs + NMP as function of the composition expressed in the mole fraction (x_1) of IL for (a) TMAH (1) + NMP (2), (b) TEAH (1) + NMP (2), (c) TPAH (1) + NMP (2), and (d) TBAH (1) + NMP (2) at (○) 25, (Δ) 30, (□) 35, and (●) 40 °C at atmospheric pressure. The solid line represents the smoothness of these data.

2.3.3. Ultrasonic Sound Velocity Measurements. A single crystal ultrasonic interferometer (model F-05) from Mittal Enterprises, New Delhi, India, at 2 MHz frequency was used for sound velocity measurements for pure solvents and mixtures at various temperatures. Prior to measurements, the interferometer was calibrated with double distilled water and purified methanol. A thermostatically controlled, well-stirred circulating water bath with a temperature controlled to ±0.01 K was used for all of the ultrasonic sound velocity measurements for pure components and mixtures. The uncertainty of the sound velocity is 0.02%.

2.3.4. Viscosity Measurements. Vibro viscometer (model SV-10, A&D Company Limited, Japan) was used for viscosity measurements. The instrument has been provided with two sensor plates of gold coating. The measurements of η were taken from the digital display device attached to the vibro viscometer. Viscosity measurements of the sample were taken at heating rate 1 °C/15 min for getting the thermodynamic equilibrium. Viscometer was calibrated with pure water and purified methanol at various temperatures. A thermostatically controlled, well-stirred circulated water bath with a temperature controlled to ±0.01 °C was used for all the viscosity measurements. Typically, the viscosities uncertainty is to be 1%.

2.3.5. Hydrogen Bonding Through Simulation Program. The structures of ILs and of NMP were optimized based on molecular mechanics and semiempirical calculations using the HyperChem 7 Molecular Visualization and Simulation program. Geometry optimizations based on molecular mechanics (using the MM + force field) and semiempirical calculations were used to find the coordinates of molecular structures that represent a potential energy minimum. For geometry optimization using both molecular mechanics and semiempirical calculations, the Polak-Ribiere routine with rms gradient of 0.01 as the termination condition was used. The minimum distance between solvent molecules and solute atoms was set at 2.3 Å. Molecular dynamics calculations were used to obtain a lower energy minimum by enabling molecules to cross potential barriers.[15,41−43] The structures of ILs were optimized using semiempirical calculations, and single-point calculations were carried out to determine the total energy and heat of formation.

3. RESULTS AND DISCUSSION

Virtually, the thermophysical properties of ILs mainly depend on the nature and structure of ions and the alkyl chain length of the cation. As it can be seen in Figure 2, ρ, u, and η values of ILs have been found to decrease linearly with increasing the temperature. Further, the ρ and u values decrease as the cation alkyl chain length increases from methyl to butyl while an opposite trend was observed, in which the values of η increase

dx.doi.org/10.1021/jp3015386 | J. Phys. Chem. B 2012, 116, 4561−4574

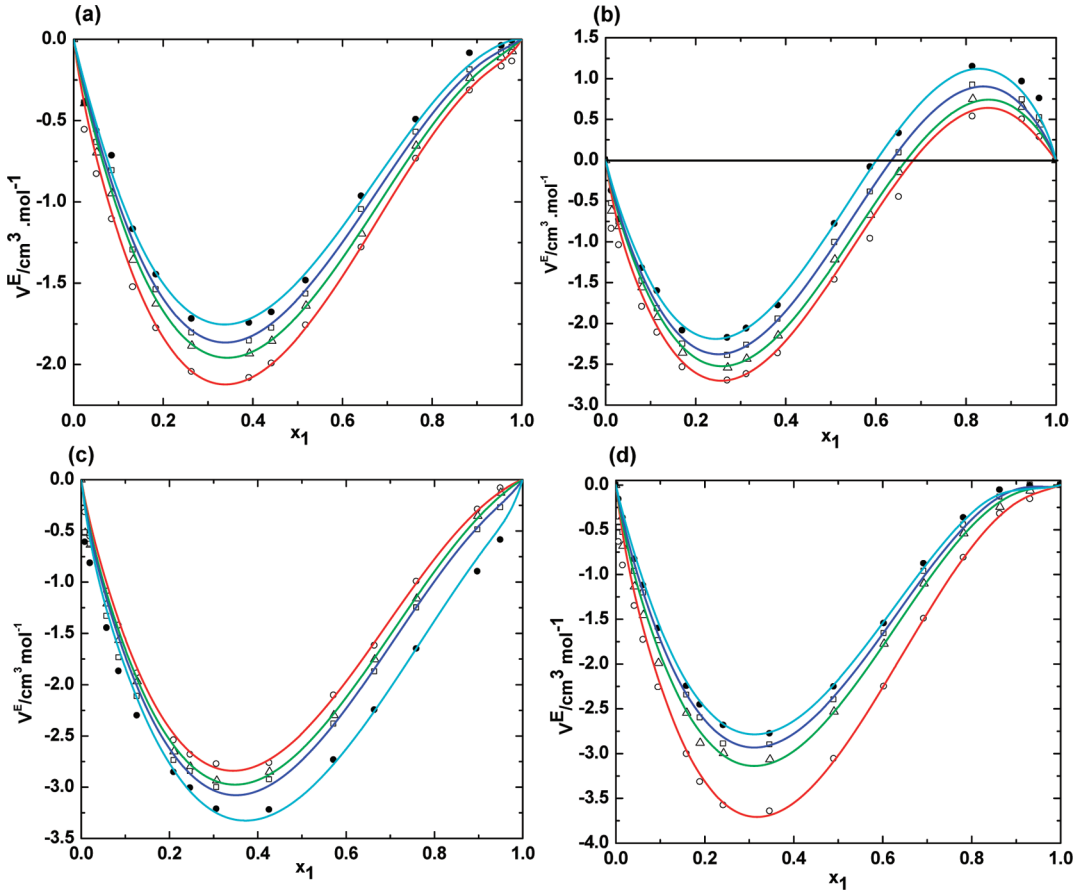

Figure 6. Excess molar volumes (V^E) for the mixtures of ILs + NMP as function of the composition expressed in the mole fraction (x_1) of IL for (a) TMAH (1) + NMP (2), (b) TEAH (1) + NMP (2), (c) TPAH (1) + NMP (2), and (d) TBAH (1) + NMP (2) at (○) 25, (Δ) 30, (□) 35, and (●) 40 °C at atmospheric pressure. The solid lines correlated by Redlich−Kister equation.

with increasing the number of carbon atoms in the alkyl chain length of cation of ILs. This is mainly contributing to anion accommodation closer to the cation. These observed results are quite consistent with the existing results,[44−46] in which ρ and u values decrease while η values increase with increasing the cation alkyl chain length of ILs. Apparently, ILs that possess a higher cation side chain are accompanied by lower ρ, lower u, and larger η. Clearly, our results might imply that the cation size was responsible for the alteration of the thermophysical properties of protic ILs.

When the number of carbon atoms in the alkyl chain length of the cation is increased, the change in investigated properties is very high from methyl to propyl group of ILs. However, not much difference was observed in ρ, u and η values among higher alkyl chain length of cation of ILs from TPAH to TBAH (Figure 2). Obviously, this phenomena agrees well with recent reports that show the thermophyiscal properties higher for cation size of ILs are not much altering.[47,48] The highest η of the IL containing the $[TBA]^+$ cation can be explained by strong molecular interactions due to hydrogen bonding. The lower η of the $[TMA]^+$ IL can be explained by the charge delocalization in the $[OH]^-$anion combined with a low molecular weight and size of the IL. The highest viscosity found for TBAH having the highest molecular weight of all ILs studied within this work. Usually, low η values for ILs where the cation has a sufficient side chain mobility and a low molecular weight of IL.[28,49]

Figures 3−5 and Table 1S reveal the measured values for the temperature dependence properties ρ, u, and η for a series of ammonium hydroxide ILs, TMAH, TEAH, TPAH, TBAH, and NMP, as well as their mixtures as a function of IL concentration for complete composition range at temperatures from 25 to 40 °C in steps of 5 °C under atmospheric pressure. Since, NMP has high dielectric constant (ε = 32.2 at T = 298.15 K),[21] we have obtained complete miscible solutions with all studied ILs. These results allow us to analyze the influence of alkyl chain length of cation of IL and temperature on the mixed solvents of IL with NMP. Therefore, the effect of the ILs on ρ, u, and η in the NMP has been examined as a function of temperature. Figure 3a illustrates that with the addition of IL to NMP a significant increase in ρ occurs for the mixtures of TMAH + NMP up to ∼0.3000 at all experimental temperatures. A drastic decrease in ρ was found in this mixture as the mole fraction of IL increases above ∼0.4500 at all temperatures, as shown in Figure 3a. This may be due to a decrease in the ion pair interactions between TMAH and NMP. The observed behavior of ρ for the system TEAH + NMP is a sharp increase up to ∼0.2000 mol fraction of TEAH after an abrupt decrease up to the mole fraction ∼0.8100. Eventually, a slight increase in the value of ρ was found for the remaining IL-rich region (Figure 3b). Within the TPAH + NMP mixture the ρ values increase significantly upon increasing the mole fraction of TPAH up to ∼0.2100, and later drastic decrease in ρ was found in this mixture of IL at all studied temperatures, as shown in the Figure 3c. The ρ values for the mixture of TBAH in NMP increase

dx.doi.org/10.1021/jp3015386 | J. Phys. Chem. B 2012, 116, 4561−4574

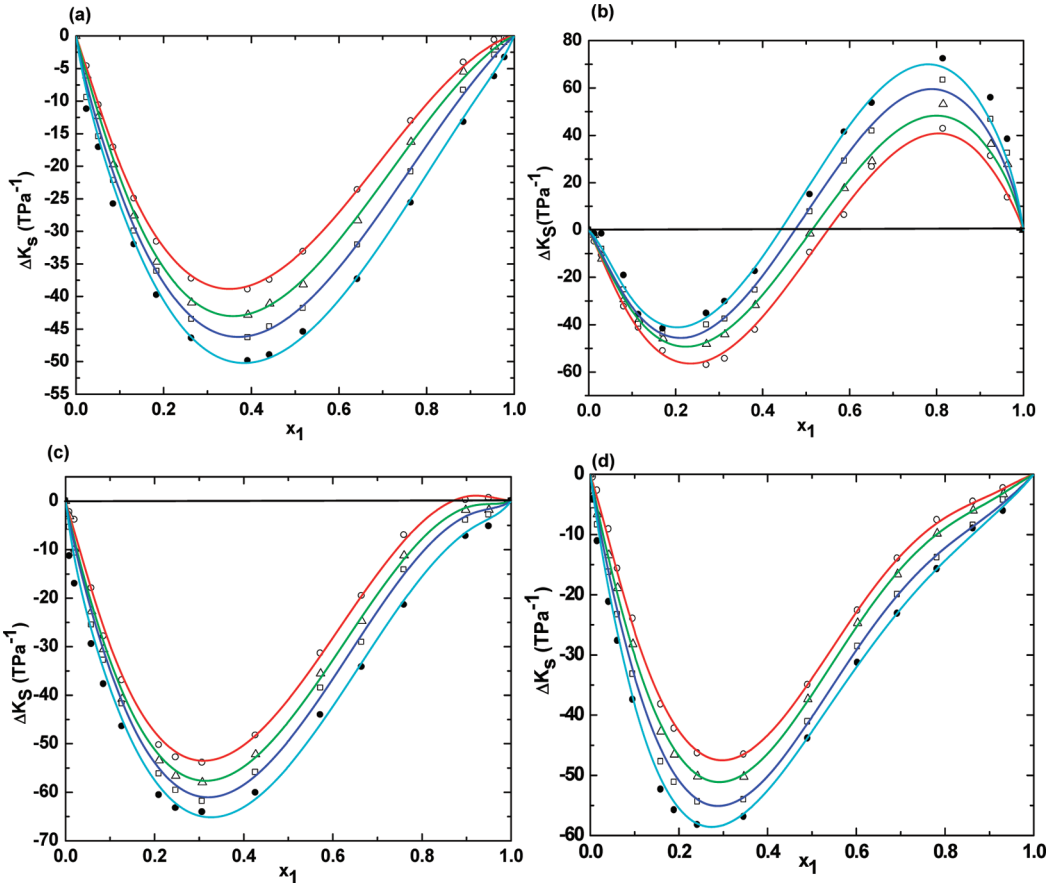

Figure 7. Deviation in isentropic compressibility ($\Delta\kappa_s$) for the mixtures of ILs + NMP as function of the composition expressed in the mole fraction (x_1) of IL for (a) TMAH (1) + NMP (2), (b) TEAH (1) + NMP (2), (c) TPAH (1) + NMP (2), and (d) TBAH (1) + NMP (2) at (○) 25, (Δ) 30, (□) 35, and (●) 40 °C at atmospheric pressure. The solid lines correlated by Redlich−Kister equation.

gradually up to ∼0.1900 mol fraction of TBAH after an abruptly decrease in the value for the rest of mole fraction of TBAH (Figure 3d). The measured ρ results in Figure 3 explicitly elucidate that the ρ values significantly decrease as the temperature increases in all four systems. As can be seen from Figure 3, the lower alkyl chain lengths of cations of ILs are much denser than higher alkyl chain lengths of ILs.

The temperature-dependent u values of ILs with NMP show different behavior for each system as displayed in Figure 4. For the TMAH with NMP system, a monotonic increase is observed when the TMAH concentration increases in the mixture at all studied temperatures as illustrated in Figure 4a. The opposite behavior is observed for the TEAH with NMP system, in which, the u values sharply increase up to ∼0.3000. Later, the values of u decrease with increasing the mole fraction of TEAH up to ∼0.8100, and finally a sharp increase occurs above the mole fraction ∼0.8100 at all studied temperatures, as shown in Figure 4b. On the other hand, Figure 4c show that the values of u were found to increase initially with increasing the mole fraction of TPAH in NMP system up to ∼0.5700, and afterward the u values sharply decrease up to ∼0.9000. From ∼0.9000 onward the u value increases at all experimental temperatures. With an increase in the concentration of TBAH in the mixture of TBAH + NMP, u values initially increase rapidly up to ∼0.3400 of IL, and later the u values slightly increase for the remaining composition of TBAH at all investigated temperatures (Figure 4d). Depending on the mixture composition, a different type of influence of the cation can be observed. So, for NMP-rich composition, the u values increase, whereas for the majority of IL compositions, the behavior is the opposite. As shown in Figure 4, the u values decrease with increasing the temperature in all ILs studied systems.

To explain the effect of the alkyl chain length of the cation on the $[R_4N]^+[OH]^-$ and further to gain deeper insight into the mechanism present within ILs with NMP, we have also measured the η values for ILs with NMP under the same experimental conditions. The experimental data are presented in Figure 5 as a function of IL concentrations at different temperatures. An increase in η is observed when TMAH composition enhances in mixture of TMAH with NMP at all studied temperatures. This result has been interpreted by the fact that the strong columbic interaction between the ions is strengthening upon mixing with the organic solvent leading to a lower mobility of the ions. Analogously, the η values for the mixture of TEAH or TPAH + NMP increase rapidly up to ∼0.5000 or ∼0.4000 mol fraction of TEAH or TPAH, respectively. Later and abrupt, slight increase is observed for the rest of the IL composition, whereas in the case of TBAH with NMP, the η values increase rapidly until the mole fraction of IL is ∼0.4000 and then slightly increase with further addition of IL at all studied temperatures, as shown in Figure 5d.

Further, at a given temperature, the η value of the TMAH + NMP mixture is found to be lower than those of TEAH, TPAH, and the TBAH + NMP system. Clearly, the η values increased with increasing the number of carbon atoms in the alkyl chain and are likely to be influenced by cation size.

dx.doi.org/10.1021/jp3015386 | J. Phys. Chem. B 2012, 116, 4561−4574

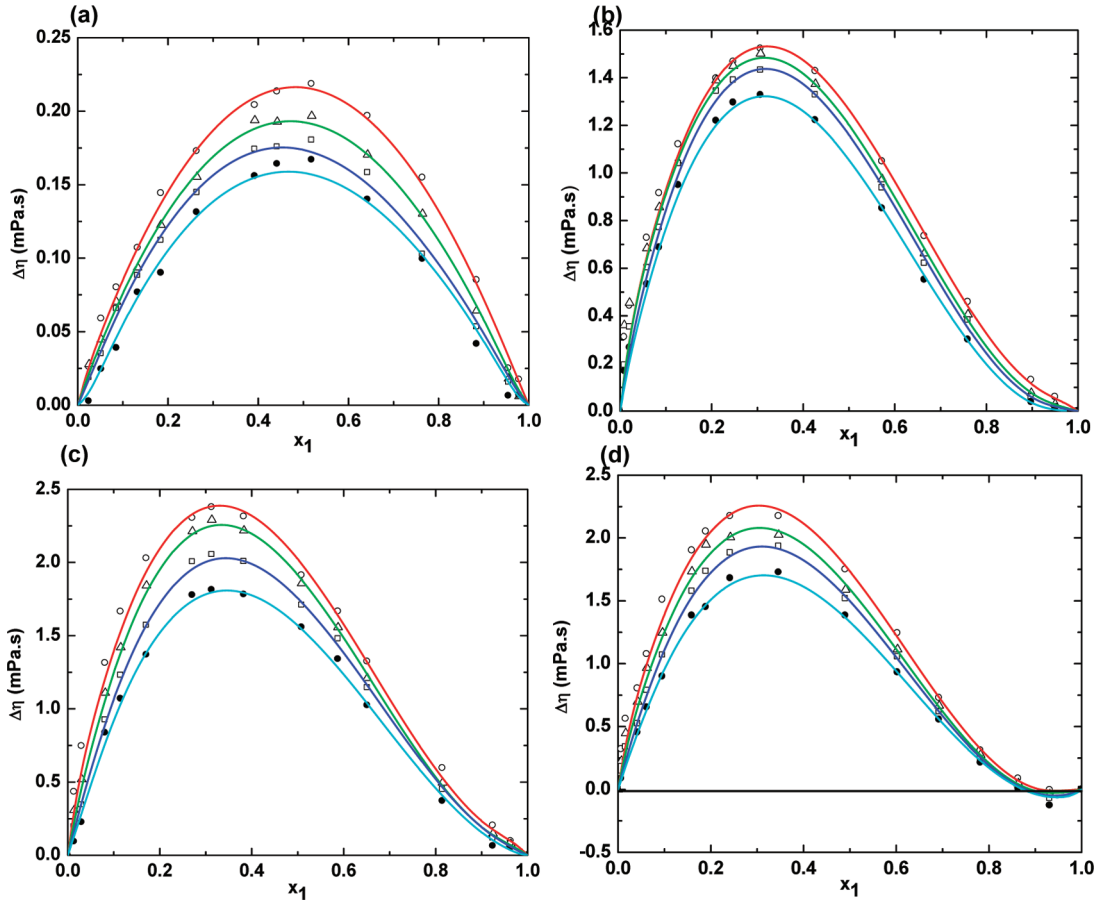

Figure 8. Deviation in viscosity ($\Delta\eta$) for the mixtures of ILs + NMP as function of the composition expressed in the mole fraction (x_1) of IL for (a) TMAH (1) + NMP (2), (b) TEAH (1) + NMP (2), (c) TPAH (1) + NMP (2), and (d) TBAH (1) + NMP (2) at (○) 25, (Δ) 30, (□) 35, and (●) 40 °C at atmospheric pressure. The solid lines correlated by Redlich–Kister equation.

However, in the case of TPAH or TBAH with NMP, the columbic interactions strengthen as the concentration of IL is increased, and thereby the viscosity is high at all investigated concentrations. We have suspect the reason for the high viscosity in the case of TPAH or TBAH is that the size of cation is large enough to facilitate the interactions between anion and cation instead of between IL and molecular liquid. On the other hand, due to the large gap in the size of anion and cation of TMAH the interactions are not enough to enhance the viscosity values. However, interestingly temperature shows similar effect on all binary mixtures. One can clearly understand from Figure 5 that, in all investigated binary systems, η decreases as the temperature increases. This mainly contributes to the weak coulomb interactions, and thereby, the mobility of ions increases and ultimately η values are decreased.

Excess molar volume (V^E) deviation in isentropic compressibility ($\Delta\kappa_s$) and the deviation in viscosities ($\Delta\eta$) were evaluated from the experimental data according to well-known thermodynamic expressions.[13,24] Isentropic compressibility (κ_s) was calculated from Laplace equation. The composition dependence of the V^E, $\Delta\kappa_s$, and $\Delta\eta$ properties represents the deviation from ideal behavior of the mixtures and provides an indication of the interactions between IL and NMP. The values of V^E, $\Delta\kappa_s$, and $\Delta\eta$ for the binary mixtures at various temperatures as function of ILs concentrations are included in Table 1S. Figures 6–8 display the values of V^E, $\Delta\kappa_s$, and $\Delta\eta$, respectively, along with the fitted curves for the NMP with ILs as function of IL concentrations at various temperatures. Further, for the sake of clarity and presentation, the values of V^E, $\Delta\kappa_s$, and $\Delta\eta$ for IL with NMP over the whole composition range at 25 °C are graphically represented in Figure 9. These properties were correlated with composition (x) using the Redlich–Kister equation

$$Y = x_1x_2\left(\sum_{i=0}^{n} a_i(x_1 - x_2)^i\right) \quad (1)$$

where Y refers to V^E, $\Delta\kappa_s$, or $\Delta\eta$. a_i is adjustable parameter and can be obtained by least-squares analysis. Values of the fitted parameters are listed in Table 2 along with the standard deviations of the fit.

Graphical representations in Figure 6 show that the values of V^E are negative across the complete composition range for ILs with NMP systems at all examined temperatures, except for the TEAH + NMP system. In the case of the TEAH + NMP mixture, the V^E values reveal an inversion in the sign from negative to positive deviation. The negative excess molar volumes reveal that the systems have a strong packing effect by hetero-associations between both molecules through H-bonding. The structural changes upon mixing are remarkable for IL and NMP, considering that, despite the dipolar ordering in their pure compounds, H-bonding is only developed in the presence of IL molecules. As can be seen in Figure 6a, the V^E values for TMAH + NMP are negative in the entire range of composition, at all temperatures. It approaches the minimum values in the NMP-rich region for the TMAH + NMP system at mole

dx.doi.org/10.1021/jp3015386 | J. Phys. Chem. B 2012, 116, 4561–4574

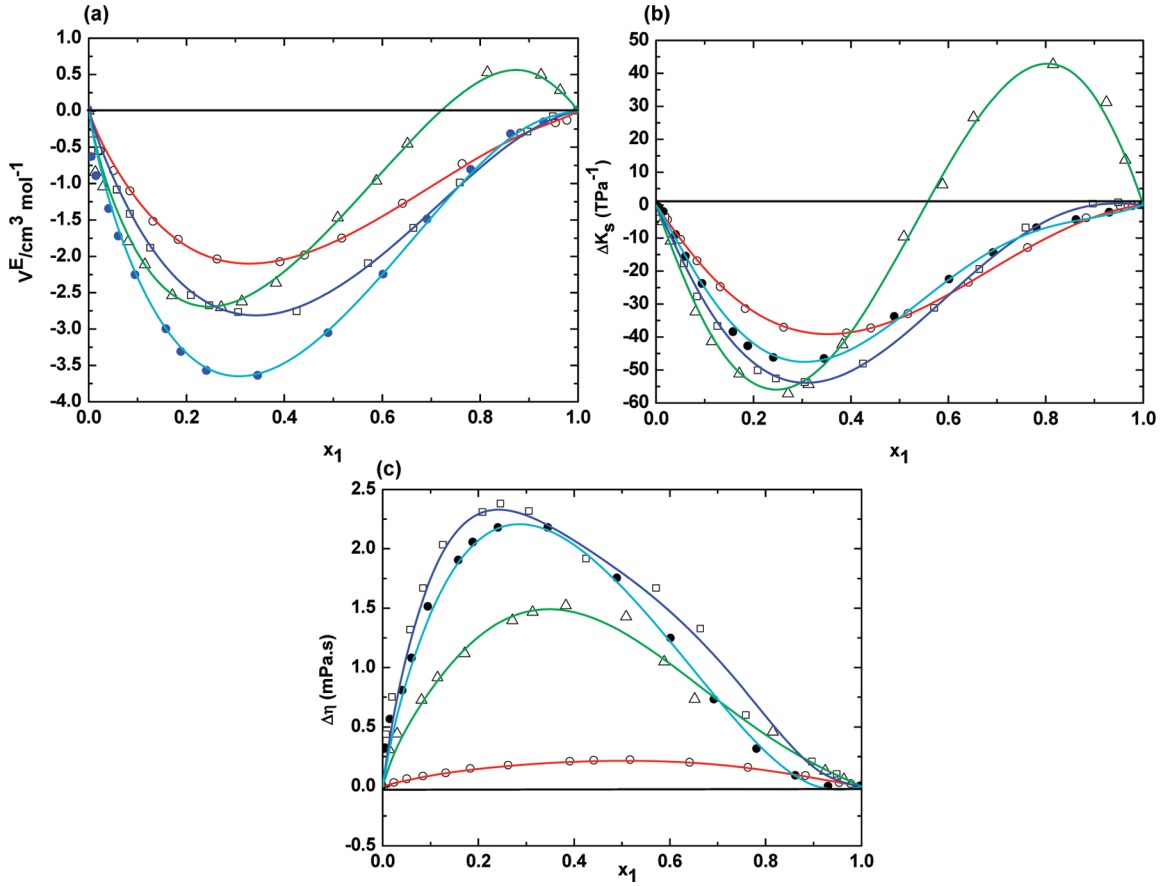

Figure 9. Plot of (a) excess molar volumes (V^E), (b) deviation in isentropic compressibility ($\Delta\kappa_s$), and (c) deviation in viscosity ($\Delta\eta$) for the mixtures of (○) TMAH (1) +, (Δ) TEAH (1) +, (□) TPAH (1), or (●) TBAH (1) + NMP (2) as function of the composition expressed in the mole fraction (x_1) of IL at 25 °C under atmospheric pressure. The solid lines represent the fit of the experimental data by Redlich−Kister equation.

fractions of TMAH about $x_1 \approx 0.39000$ at all investigated temperatures. This behavior can be explained in terms of hydrogen bonding that is certainly more-dependent than columbic interactions. The minimum decreases in V^E as the temperature increases for the TMAH + NMP system, and this can be due to hydrogen bonds between molecules and IL. This phenomenon is explicitly explained in Scheme 1. The negative excess molar volumes reveal that a more efficient packing or attractive interactions occurred when the TMAH mixed with NMP. The interactions between the NMP molecules and the ions of these TMAH are due to ion−dipole interactions. This will reduce the hydrogen bond between the cation and anion in the IL, which contribute to the negative V^E values.

In other words, the results in Figure 6b depict that an inversion in the sign from negative to positive deviation in the V^E values was observed for the TEAH + NMP mixture, which implies that the interactions between IL and NMP decrease as the concentration of the IL increases. Moreover, the V^E values are positive for IL-rich compositions and negative for NMP-rich compositions for the mixture of TEAH + NMP at all investigated temperatures (Figure 6b). Decrease in the magnitude of the negative V^E values with an increase in IL composition can be attributed to the decrease of hydrogen bonding. Although it can also be understood as an increase in the concentration of the IL, a decrease of packing efficiency between NMP and IL contributes to a positive deviation. The minimum value occurs at the mole fraction of about ∼0.2700 and maximum at ∼0.8100 for the system TEAH + NMP at all investigated temperature. The absolute minimum decreases while the maximum increases with an increase of temperature in this system. It is noteworthy to compare the negative deviation of excess volumes of TMAH + NMP with that of TEAH + NMP, suggesting that there is a difference of the alkyl chain in the TEAH, leading to variation in the hydrogen bonding.

The values of V^E for TPAH with NMP are negative in the entire range of composition, at various temperatures. It approaches the minimum values in the TPAH + NMP system at mole fractions of this IL of about $x_1 \approx 0.3300$ at all investigated temperatures, as seen in Figure 6c. This behavior can be explained in terms of hydrogen bonding that is certainly more T-dependent than columbic interactions. From close observation of Figure 6d, one can clearly see that the values of V^E for NMP with TBAH are negative over the whole concentration range at all investigated temperatures. This might be due to the large difference between molar volumes of the NMP and TBAH imply that it is possible that the relatively small organic molecules fit into the interstices upon mixing at all studied temperatures. Therefore, the filling effect of molecular liquids in the interstices of ILs, and the ion-dipole interactions between organic molecular liquid and ILs, all contribute to the negative values of V^E. On the other hand, the TBAH + NMP mixture reveals negative values of V^E and minimum at ∼0.3200 as seen in Figure 6d. The minimum can be due to hydrogen bonds between molecules and IL.

The negative V^E values reveal that a more efficient packing or attractive interaction occurred when these IL and NMP were

dx.doi.org/10.1021/jp3015386 | J. Phys. Chem. B 2012, 116, 4561−4574

Table 2. Estimated Parameters of eq 1 and Standard Deviation, σ, for the Systems of ILs with NMP as Function of Temperature

Y	system	T/°C	a_0	a_1	a_2	a_3	a_4	σ
V^E/ cm^3 mol^{-1}	TMAH + NMP	25	−7.182	6.603	−2.262			0.060
		30	−6.760	6.092	−0.862			0.054
		35	−6.453	6.102				0.004
		40	−6.105	5.999	0.785			0.005
	TEAH+ NMP	25	−6.198	13.592	−2.931	7.644		0.144
		30	−5.301	14.911	−0.089	4.913		0.008
		35	−4.401	15.506	−0.512	4.223		0.007
		40	−3.586	15.966	1.775	4.355		0.008
	TPAH + NMP	25	−9.839	7.945	−1.017	2.531		0.006
		30	−10.366	7.291	−1.919	4.291		0.010
		35	−10.978	7.231	1.901	4.199	−9.017	0.008
		40	−12.372	6.312	3.555	2.951	−16.185	0.101
	TBAH+ NMP	25	−12.215	12.293	3.585	4.731	−12.230	0.139
		30	−9.971	11.490	−2.734	2.995	−10.115	0.008
		35	−9.420	11.749	2.323	0.810	−6.042	0.007
		40	−8.696	11.580	−0.471			0.002
ΔK_s/ T.Pa^{-1}	TMAH + NMP	25	−138.67	117.43	−17.36			0.4
		30	−155.81	119.63	9.19			0.3
		35	−169.97	96.92	−11.48	−43.952		0.6
		40	−184.38	102.68	−54.00			1.2
	TEAH+ NMP	25	−58.72	544.05	69.44	−7.470		1.7
		30	−16.20	486.65	−34.69	105.16	260.10	1.8
		35	24.84	512.87	−50.28	153.02	349.79	2.1
		40	67.06	543.43	−126.43	151.48	568.17	3.0
	TPAH + NMP	25	−163.36	250.12	−3.89	−60.32		1.2
		30	−178.23	228.38	−37.05			0.7
		35	−192.54	227.80	−51.06			1.1
		40	−206.87	220.53	−110.01			2.7
	TBAH+ NMP	25	−228.98	261.97	−55.33	−92.62		1.0
		30	−251.64	247.54				2.0
		35	−278.71	259.77	54.93	31.82	−134.82	1.3
		40	−286.84	260.22	−82.56	84.53		3.2
$\Delta\eta$/ mPa.s	TMAH + NMP	25	−0.86	0.003	0.006	−0.276		0.003
		30	−0.78	−0.037	−0.102	−0.219		0.003
		35	−0.716	−0.009	−0.151	−0.161		0.002
		40	0.654	−0.009	−0.007	−0.004	−0.375	0.004
	TEAH+ NMP	25	4.84	−4.52	2.13	−2.82		0.007
		30	4.96	−5.91				0.107
		35	4.51	−5.515	1.29			0.004
		40	4.16	−5.218	0.76			0.003
	TPAH + NMP	25	−8.01	−6.88	−0.18	−3.13	5.85	0.005
		30	−7.57	−7.52	1.32			0.003
		35	7.06	−6.39				0.002
		40	−6.38	−5.68	−0.76			0.003
	TBAH + NMP	25	6.64	−7.99	2.54	−4.30		0.008
		30	6.17	−7.95	1.73	−2.58		0.005
		35	6.04	−8.21				0.003
		40	5.45	−7.19	−0.69			0.002

mixed at all cases. The interactions between the NMP molecules and the ions of IL are due to ion−dipole interactions. The observed negative V^E values for the mixture of higher alkyl chain length of IL + NMP are higher than those for lower alkyl chain length of IL + NMP under same experimental conditions. Therefore, higher alkyl chain length of cation ILs interacts with NMP more strongly than lower alkyl chain length of IL. Thus, it is important to note that the nature of interactions in the IL + NMP system is highly dependent on the alkyl chain length of IL. Interestingly, Figures 10−13 demonstrate the hydrogen bonding between ILs and NMP clearly appearing, through the semiempirical calculations which we predicted with the help of Hyperchem 7.

Figure 7 depicts the $\Delta\kappa_s$ values of ILs + NMP over the full composition range at various temperatures as a function of ILs concentration. From Figure 7a, it can be seen that $\Delta\kappa_s$ values are negative over the whole composition range and at all experimental temperatures for TMAH + NMP systems. The minimum values are observed at mole fraction ∼0.4000 for the TMAH + NMP system. The negative $\Delta\kappa_s$ values of TMAH + NMP are attributed to the strong attractive interactions due to the solvation of the ions in these solvents. An inversion in the

dx.doi.org/10.1021/jp3015386 | J. Phys. Chem. B 2012, 116, 4561−4574

Scheme 1. Schematic Depiction of the Hydrogen Bonding Interactions between ILs + NMP for the Negative Deviation

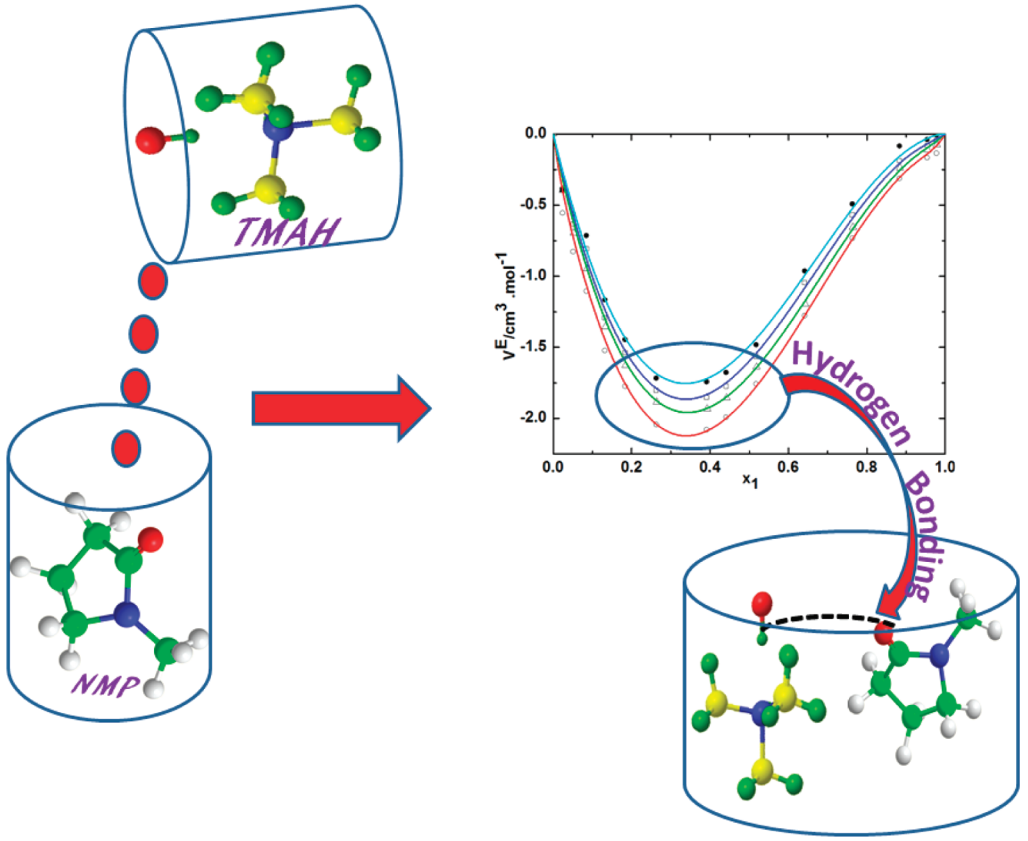

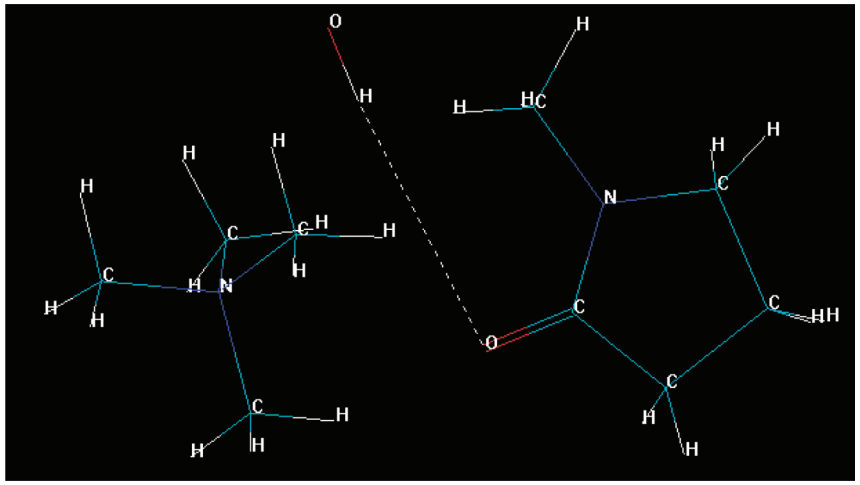

Figure 10. Hydrogen bonding interaction between TMAH and NMP molecules, which is predicted by semiempirical calculation with the help of Hyperchem 7.

sign of $\Delta\kappa_s$ values from negative to positive is observed for the TEAH + NMP system at all investigated temperatures (Figure 7b). As the concentration of the IL increases and a large portion of the NMP molecules are solvated, the amount of bulk solvent decreases causing a decrease in the compressibility. As the mole fraction increases, the negative deviation increases up to ~0.2700, while on further addition of the IL, there is decrease in the compressibility, and it enters into positive deviation and has a maximum value at the mole fraction of ~0.8100 at all temperatures.

The curves in Figure 7c,d show that the $\Delta\kappa_s$ values for the TPAH or TBAH + NMP systems are negative over the complete composition range and at all temperatures employed (except TPAH at higher IL composition and at low temperature). The minimum is approached at mole fractions of ~0.3000 and ~0.3200 for the TPAH + NMP and TBAH + NMP systems, respectively. The negative $\Delta\kappa_s$ values attributed to the strong attractive interactions due to the salvation of the ions in these solvents. The negative values of $\Delta\kappa_s$ of the IL with NMP imply that solvent molecules around solute are less compressible than the solvent molecules in the bulk solutions. While on further addition of IL there is a decrease in the compressibility graph at all temperature ranges. This might be due to decrease in attraction of NMP and IL molecules in IL rich concentration region. These discrepancies vary from IL to IL

dx.doi.org/10.1021/jp3015386 | J. Phys. Chem. B 2012, 116, 4561−4574

and solvent to solvent and also depend on the nature as well as structural arrangement of IL and solvent.

An examination of the curves in Figure 8 shows that the $\Delta\eta$ values for ILs + NMP are positive as a function of temperature except for TBAH + NMP in the very IL-rich region, in which slightly negative values are observed. The deviations are observed to be slightly negative between the mole fractions of 0.9300 and 1.000 at all experimental temperatures for the TBAH (Figure 8d). The positive deviation is characteristic of mixtures containing hydrogen bonding between ions of IL and NMP molecules (Scheme 1). The positive values of $\Delta\eta$ for the investigated binary systems suggest that the η values of associates formed between unlike molecules are relatively more than those of the pure component. According to Bearman and Jones,[50] the η of a mixture depends strongly on its entropy, which is related to the liquid's structure. Therefore, the $\Delta\eta$ value depends on molecular interactions as well as on the size and shape of the molecules. The highest $\Delta\eta$ was observed for TBAH with NMP at all studied temperatures. These variations in $\Delta\eta$ could be attributed to relatively larger hydrogen bonding interactions of the ion with NMP as compared with the rest of the ions of IL with NMP. The minimum $\Delta\eta$ values were observed in the case of TMAH with NMP, as this system contains more van der Walls interactions. Indeed, the temperature strongly influences the $\Delta\eta$. As the temperature increases, the $\Delta\eta$ values were decreased for all of the investigated systems, and this reveals that the interactions become very weak due to weakening of the dipolar association by the IL as well as the dissociation of the IL ion pair. These results are well corroborated with the V^E and $\Delta\kappa_s$ data that as the alkyl chain increases the hydrogen bonding increases.

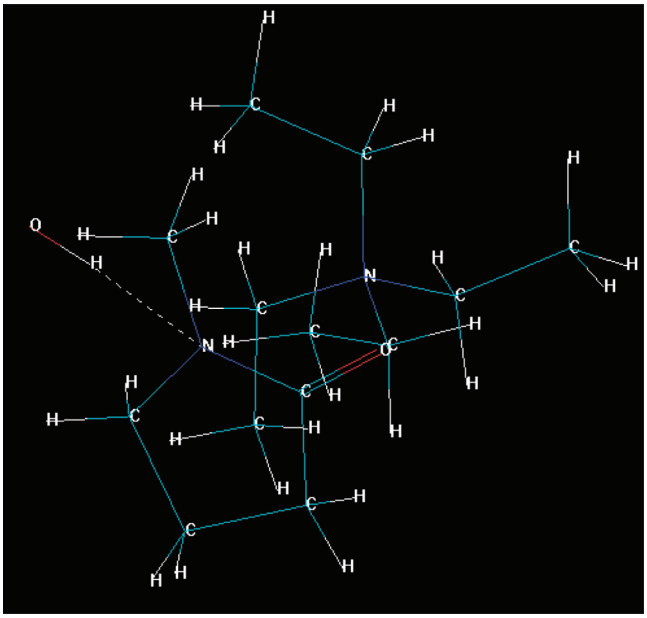

Figure 11. Hydrogen bonding interaction between TEAH and NMP molecules, which is predicted by semiempirical calculation with the help of Hyperchem 7.

In Figure 9a, it can be observed that the negative V^E values increase with increasing alkyl chain length of IL. Clearly, the negative V^E values for the mixture of higher alkyl chain length of IL + NMP are higher than those for lower alkyl chain length of IL + NMP at 25 °C. Therefore, it is important to note that the nature of interactions in the IL + NMP system is highly dependent on the alkyl chain length of IL. It is interesting to note that the $\Delta\kappa_s$ values in the TEAH + NMP mixture show more negative values at the NMP-rich composition than the rest of the mixtures at 25 °C (Figure 9b). Furthermore, the observed positive values at IL-rich compositions show that there exists no specific interactions between unlike molecules and also that the compact structure of the polar component (NMP) due to dipolar association has been broken by the

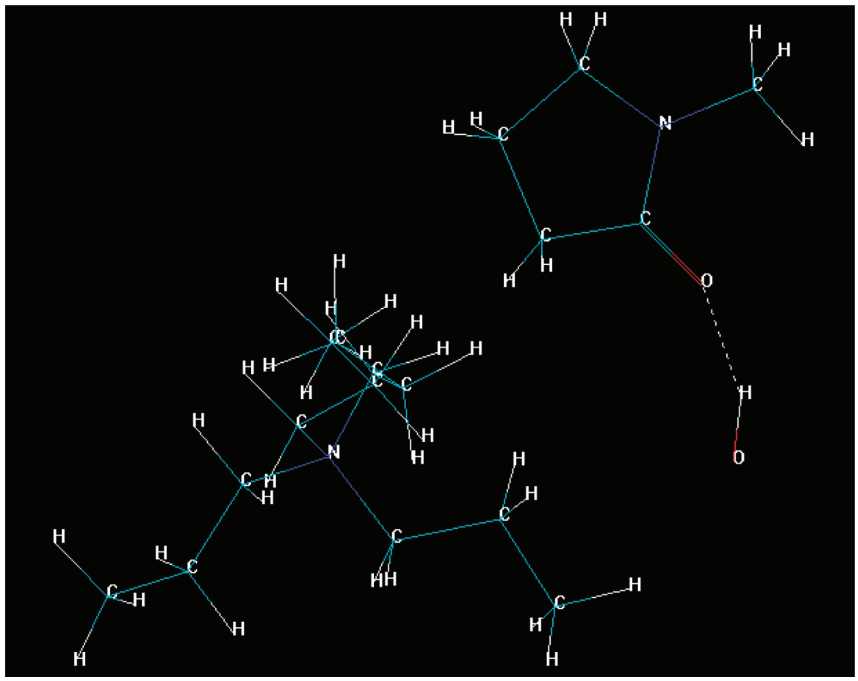

Figure 12. Hydrogen bonding interaction between TPAH and NMP molecules, which is predicted by semiempirical calculation with the help of Hyperchem 7.

dx.doi.org/10.1021/jp3015386 | J. Phys. Chem. B 2012, 116, 4561−4574

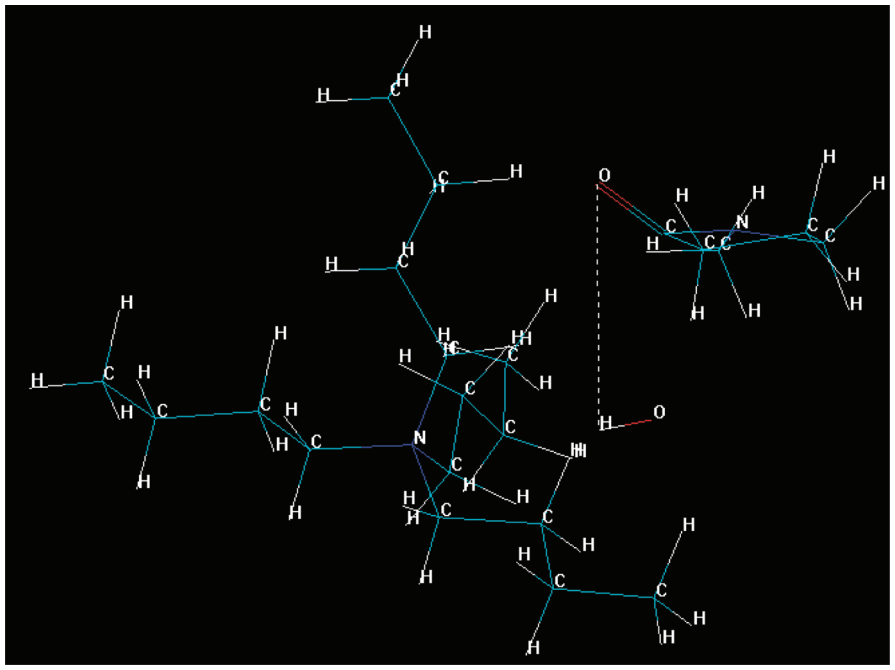

Figure 13. Hydrogen bonding interaction between TBAH and NMP molecules, which is predicted by semiempirical calculation with the help of Hyperchem 7.

TEAH. This conclusion is consistent with the V^E data in the case of the TEAH system. The curves in Figure 9b show that the $\Delta\kappa_s$ values for the TMAH, TPAH, or TBAH + NMP systems are negative over the whole composition range at 25 °C (except TPAH at higher IL composition). The results in Figure 9c show that the $\Delta\eta$ values for ILs + NMP are the positive at 25 °C except for TBAH + NMP at the very IL-rich region, in which a slightly negative value observed. The $\Delta\eta$ values increase with increasing the alkyl chain length of the cation of IL, except in the case of the TBAH system at 25 °C.

4. CONCLUSIONS

This work reports extensive experimental data of thermophysical properties of four ammonium based ILs as a function of temperature. Further, to obtain some insight into new generation of green solvents, we synthesized the novel ammonium hydroxide ILs namely TMAH, TEAH, TPAH, and TBAH and studied the influence of IL on the polar solvent, NMP. Variable temperature measurements for ρ, u, and η for ILs with NMP are performed changing the temperature from 25 to 40 °C in steps of 5 °C under room pressure. From these measurements, we have predicted V^E, $\Delta\kappa_s$, and $\Delta\eta$ at each temperature as a function of IL concentration. The predicted properties were correlated with the Redlich−Kister type equation. Obviously, fascinating results are obtained for structure-based and temperature-dependent properties of novel kinds of ILs with NMP, and the data reveals that higher alkyl chain ILs have a greater tendency to form hydrogen bonds as compared to lower alkyl chain ILs. These observed interactions are supported by our theoretical calculations, which are obtained by Hyperchem 7.

■ ASSOCIATED CONTENT

Ⓢ Supporting Information

The values of V^E, $\Delta\kappa_s$, and $\Delta\eta$ for the binary mixtures at various temperatures as function of ILs concentrations (Table 1S). This material is available free of charge via the Internet at http://pubs.acs.org.

■ AUTHOR INFORMATION

Corresponding Author

*E-mail: venkatesup@hotmail.com; pvenkatesu@chemistry.du.ac.in. Tel: +91-11-27666646-142. Fax: +91-11-2766 6605.

Notes

The authors declare no competing financial interest.

■ ACKNOWLEDGMENTS

We gratefully acknowledge the Council of Scientific Industrial Research (CSIR), New Delhi, through Grant No. 01(2343)/09/EMR-II, the Department of Science and Technology (DST), New Delhi, India (Grant No. SR/SI/PC-54/2008), and University Grants Commission (UGC), New Delhi for financial support.

■ REFERENCES

(1) Seddon, K. R. *J. Chem. Technol. Biotechnol.* **1997**, *68*, 351−356.
(2) Welton, T. *Chem. Rev.* **1999**, *99*, 2071−2084.
(3) Greaves, T. L.; Drummond, C. J. *Chem. Rev.* **2008**, *108*, 206−237.
(4) Rogers, R. D.; Seddon, K. R. *Science* **2003**, *302*, 792−793.
(5) Davis, J. H. *Chem. Lett.* **2004**, *33*, 1072−1077.
(6) Attri, P.; Venkatesu, P.; Kumar, A. *Phys. Chem. Chem. Phys.* **2011**, *13*, 2788−2796.
(7) Plechkova, N. V.; Seddon, K. R. *Chem. Soc. Rev.* **2008**, *37*, 123−150.
(8) Attri, P.; Venkatesu, P. *Phys. Chem. Chem. Phys.* **2011**, *13*, 6566−6575.
(9) Earle, M. J.; Esperanca, J.; Gilea, M. A.; Lopes, J. N. C.; Rebelo, L. P. N; Magee, J. W.; Seddon, K. R.; Widegren, J. A. *Nature* **2006**, *439*, 831−834.
(10) Henderson, L. C.; Byrne, N. *Green Chem.* **2011**, *13*, 813−816.
(11) Constantinescu, D.; Weingärtner, H.; Herrmann, C. *Angew. Chem., Int. Ed.* **2007**, *46*, 8887−8889.
(12) Attri, P.; Reddy, P. M.; Venkatesu, P. *Indian J. Chem. A* **2010**, *49A*, 736−742.
(13) Attri, P.; Reddy, P. M.; Venkatesu, P.; Kumar, A.; Hofman, T. *J. Phys. Chem. B* **2010**, *114*, 6126−6133.

(14) Attri, P.; Venkatesu, P.; Kumar, A. *J. Phys. Chem. B* **2010**, *114*, 13415−13425.
(15) Attri, P.; Venkatesu, P.; Hofman, T. *J. Phys. Chem. B* **2011**, *115*, 10086−10097.
(16) Reddy, P. M.; Venkatesu, P. *J. Phys. Chem. B* **2011**, *115*, 4752−4757.
(17) Newington, I.; Perez-Arlandis, J. M.; Welton, T. *Org. Lett.* **2007**, *9*, 5247−5250.
(18) Chiappe, C.; Pomelli, C. S.; Rajamani, S. *J. Phys. Chem. B* **2011**, *115*, 9653−9661.
(19) D'Anna, F.; Marullo, S.; Noto, R. *J. Org. Chem.* **2010**, *75*, 767−771.
(20) García-Abuín, A.; Gómez-Díaz, D.; La Rubia, M. D.; Navaza, J. M. *J. Chem. Eng. Data* **2011**, *56*, 646−651.
(21) Riddick, J. A.; Bunger, W. B.; Sakano, T. K. *Organic Solvents*, 4th ed.;, Wiley-Inter Science: New York, 1986.
(22) Kumari, P. G.; Venkatesu, P.; Hsieh, C. T.; Rao, M. V. P.; Lee, M. J.; Lin, H. M. *J. Chem. Thermodyn.* **2009**, *41*, 184−188.
(23) Kumari, P. G.; Venkatesu, P.; Hofman, T.; Rao, M. V. P. *J. Chem. Eng. Data* **2010**, *55*, 69−73.
(24) Govinda, V.; Attri, P.; Venkatesu, P.; Venkateswarlu, P. *Fluid Phase Equilib.* **2011**, *304*, 35−43.
(25) Mokhtarani, B.; Sharifi, A.; Mortaheb, H. R.; Mirzaei, M.; Mafi, M.; Sadeghian, F. *J. Chem. Thermodyn.* **2009**, *41*, 323−329.
(26) Wagner, M.; Stanga, O.; Schröer, W. *Phys. Chem. Chem. Phys.* **2003**, *5*, 3943−3950.
(27) Ortega, J.; Vreekamp, R.; Marrero, E.; Penco, E. *J. Chem. Eng. Data* **2007**, *52*, 2269−2276.
(28) Fröba, A. P.; Kremer, H.; Leipertz, A. *J. Phys. Chem. B* **2008**, *112*, 12420−12430.
(29) Geppert-Rybczyńska, M.; Heintz, A.; Lehmann, J. K.; Golus, A. *J. Chem. Eng. Data* **2010**, *55*, 4114−4120.
(30) Wang, J.; Wang, H.; Zhang, S.; Zhang, H.; Zhao, Y. *J. Phys. Chem. B* **2007**, *111*, 6181−6188.
(31) Firestone, A.; Dzielawa, J. A.; Zapol, P.; Curtiss, L. A.; Seifert, S.; Dietz, M. L. *Langmuir* **2002**, *18*, 7258−7260.
(32) Law, G.; Watson, P. R. *Langmuir* **2001**, *17*, 6138−6141.
(33) Zhang, Z.; Wu, W.; Gao, H.; Han, B.; Wang, B.; Huang, Y. *Phys. Chem. Chem. Phys.* **2004**, *6*, 5051−5055.
(34) Iglesias-Otero, M. A.; Troncoso, J.; Carballo, E.; Romaní, L. *J. Chem. Eng. Data* **2008**, *53*, 1298−1301.
(35) Wang, J.; Tian, Y.; Zhao, Y.; Zhuo, K. *Green Chem.* **2003**, *5*, 618−622.
(36) Murrleta-Guevara, F.; Rodibuez, A. T. *J. Chem. Eng. Data* **1984**, *29*, 204−206.
(37) Pal, A.; Singh, Y. P. *J. Chem. Eng. Data* **1995**, *40*, 818−822.
(38) García-Abuín, A.; Gómez-Díaz, D.; La Rubia, M. D.; Navaza, J. M. *J. Chem. Eng. Data* **2011**, *56*, 646−651.
(39) Weng, J.; Wang, C.; Li, H.; Wang, Y. *Green Chem.* **2006**, *8*, 96−99.
(40) Mehnert, C. P.; Dispenziere, N. C.; Cook, R. A. *Chem. Commun.* **2002**, 1610−1611.
(41) Huq, F.; Yu, J. Q. *J. Mol. Model.* **2002**, *8*, 81−86.
(42) Jorgensen, W. L.; Chandrasekhas, J.; Madura, J. D.; Impey, R. W.; Klein, M. L. *J. Chem. Phys.* **1983**, *79*, 926−935.
(43) Schmid, E. D.; Odbek, E. *Can. J. Chem.* **1985**, *63*, 1365−1371.
(44) Xiao, D.; Hines, L. G.; Li, S. F.; Bartsch, R. A.; Quitevis, E. L.; Russina, O.; Triolo, A. *J. Phys. Chem. B* **2009**, *113*, 6426−6433.
(45) Seddon, K. R.; Stark, A.; Torres, M. J. *Clean Solvents* **2002**, *819*, 34−49.
(46) Li, S.; Bañuelos, J. L.; Guo, J.; Anovitz, L.; Rother, G.; Shaw, R. W.; Hillesheim, P. C.; Dai, S.; Baker, G. A.; Cummings, P. T. *J. Phys. Chem. Lett.* **2012**, *3*, 125−130.
(47) Aparicio, S.; Atilhan, M.; Karadas, F. *Ind. Eng. Chem. Res.* **2010**, *49*, 9580−9595.
(48) Ziyada, A. K.; Wilfred, C. D.; Bustam, M. A.; Man, Z.; Murugesan, T. *J. Chem. Eng. Data* **2010**, *55*, 3886−3890.
(49) Bonhôte, P.; Dias, A. P.; Papageorgiou, N.; Kalyanasundaram, K.; Grätzel, M. *Inorg. Chem.* **1996**, *35*, 1168−1178.
(50) Bearman, R. J.; Jones, P. F. *J. Chem. Phys.* **1960**, *33*, 1432−1438.